On the synergistic interrelation between supercavity formation through vaporous and ventilated routes

Ashish Karn [a,*], Saurabh Chawdhary [b]

[a] Department of Mechanical Engineering, School of Engineering, University of Petroleum and Energy Studies, Energy Acres, Bidholi, Dehradun, Uttarakhand 248007, India.
[b] Argonne National Laboratory, Argonne, IL 60439, USA

ABSTRACT

A supercavity can be attained via two distinct routes: vaporous and ventilated supercavitation. A vaporous supercavity is one that is obtained by the coalescence of individual vapor bubbles formed by cavitation. On the other hand, a ventilated supercavity results from the coalescence of bubbles of non-condensable gas formed through gas injection at the rear part of the cavitator. A typical strategy of operation of a supercavitating underwater vehicle entails an interplay between these two modes viz. accelerating it to a high speed using ventilation, when a natural supercavity can be sustained. This fact necessitates a systematic study of the synergistic relationship between the process of supercavity formation under these two modes. Thus, in the current work, we have systematically carried out water tunnel experiments to study the effect of vaporous and ventilated modes of supercavitation on each other during supercavity formation. The results show a systematic dependence between the relevant parameters which include the formation natural cavitation number and the formation gas entrainment coefficient. Further, the effects of change in Froude number and blockage are also reported and discussed.

© 2018 Elsevier Ltd. All rights reserved.

1. Introduction

Supercavitation, a limiting case of cavitation, occurs when the formed cavity is so large so as to entirely encompass the object which forms it. Owing to its potential application in the drag reduction of underwater vehicles, supercavitation research has gained a considerable momentum in the last decade and a significant amount of research has been conducted into different aspects of supercavitation, viz. natural supercavitation, artificial supercavitation, supercavity closures, supercavity closures, ventilation demand, supercavity control etc. (Savchenko and Savchenko, 2012; Rashidi et al., 2014). Most of these studies can be broadly categorized into studies on either natural or artificial supercavitation and have been widely discussed in the prior literature recently (Karn et al., 2015a; Serebryakov et al., 2015; Karn et al., 2016a,b; Lee et al., 2016; Cao et al., 2017; Karn and Rosiejka, 2017). A natural supercavity is a consequence of the cavitation induced by reduction in pressure at the cavitator because of high liquid velocity, whereas an artificial supercavity is formed by the coalescence of individual gas bubbles resulting from the injection of a non-condensable gas at the rear of the cavitator (Karn et al., 2016a).

There are essential similarities and differences between a vaporous and a ventilated supercavity, as reported by prior studies. One of the earliest studies in this area by Silberman and Song (1961) suggested that natural and artificial supercavities should have similar average characteristics viz. cavity length, as long as the cavitation number is the same. This has been supported by a number of other authors such as Semenenko (2001) and Zhang et al. (2007). Silberman and Song (1961) further proposed that this similarity might be exploited to generate cavities by ventilation. The benefit of obtaining supercavities through the ventilation route is that low sigma values ($\sigma < 0.1$) required for supercavity generation can be obtained at a much lower flow speed of few meters per second, which otherwise require a flow speed of over 50 m/s through a purely vaporous route (Epshtein, 1975). However, there are distinct dissimilarities between the two. As pointed out by Skidmore (2013), artificial supercavities differ from the natural supercavities in their method of gas exchange. According to Cox and Clayden (1956), supercavity rear is often a very turbulent region of flow where the contents of the cavity are entrained away. In a ventilated supercavity, the air entrainment out of the supercavity depends upon the rate of gas supply. But in the case of a natural supercavity, the loss of vapor from the rear portion is made up by the evaporation at the walls of the interface and thus there is an inexhaustible supply of vapor (Cox and Clayden, 1956;

Spurk, 2002). The recent study by Karn et al. (2016a) related the gas entrainments with the supercavity closure modes and pointed out the differences in closure mechanisms for the natural and artificial cases. Their study suggested that there is an increasing tendency to form a re-entrant jet based closure in vaporous supercavities, while a myriad number of other closure mechanisms appear in ventilated supercavities.

Thus, a natural supercavity, characterized by a re-entrant jet, is essentially vaporous, whereas an artificial (or ventilated) supercavity which is primarily composed of gas, may lead to different kinds of closure mechanisms. In a natural supercavity, the cavity pressure is usually taken to be the water vapor pressure, provided the liquid does not contain any dissolved gases. However, it is noteworthy that even in the occurrence of a ventilated supercavity, there is some contribution of a 'vaporous' component that is caused by the vapor bubbles resulting from the cavitation of the liquid at the cavitator edges. Arguably, this vaporous component of supercavitation will diminish the ventilation requirements to establish an artificial supercavity. Similarly, prior reports have ascertained that the presence of a non-condensable gas inside a single cavitation bubble reduces the rate of collapse and increases the minimum bubble volume (Brennen, 2013). This factor again facilitates the coalescence of individual vapor bubbles into a vaporous supercavity. Thus, the mutual effect of both the modes of supercavitation on each other is evident. Understanding of the synergistic relationship between vaporous and ventilated supercavitation is important, especially because the operation of a supercavitating underwater vehicle is driven by an interplay between these two distinct modes of supercavitation. For instance, a typical operational strategy of a supercavitating vehicle entails accelerating the vehicle to a high speed employing a ventilated supercavity, till a point when a natural supercavity can be sustained (Karn et al., 2016b). The formation and sustenance of natural supercavitation in a vehicle (which is the desired mode of vehicle operation under cruising conditions) again depends upon two factors: the vehicle speed and the vehicle depth below the free surface, which in turn affects the hydrostatic pressure. The physical parameters involved in these studies are incoming velocity (U), ventilation flow rate at standard conditions ($\dot{Q}_{As}$), ambient pressure (P_∞), cavity pressure (P_C) and cavitator diameter (d_C), and these are typically expressed in terms of non-dimensional parameters such as Froude number, $Fr = U/\sqrt{gd_c}$, vaporous cavitation number, $\sigma_v = (p_o - p_v)/0.5\rho U^2$ etc., where g and ρ denote gravitational acceleration and water density, respectively. In addition, for ventilated/combined supercavitation, gas entrainment coefficient, $C_{Qs} = \dot{Q}_{As}/Ud_C^2$ should also be taken into consideration.

However, it may not be always possible to extricate ventilated and natural modes of supercavitation from each other. It is possible to obtain a purely vaporous supercavity at high velocities without any ventilation, while a purely artificial supercavity can be attained by injecting non-condensable gas at low velocities, when the generation of vapor bubbles due to cavitation does not take place. Even at moderate velocities, the effect of vaporous cavity formation will be observed. This suggests that the usual nomenclature of a 'ventilated supercavity' in the literature may refer to a combined vaporous-ventilated supercavity, and not to a purely ventilated supercavity, at least for a range of operational conditions. Although it may not always be possible to obtain a purely ventilated supercavity under real conditions, it can be attained in specific experimental facilities at certain conditions, for instance by increasing the test-section pressure in a cavitation tunnel. in a typical high-speed cavitation tunnel (For e.g. see Fig. 1), the test-section pressures can be completely regulated to yield a purely natural supercavity (when the test-section pressure is lowered), a purely artificial supercavity (when the test-section pressure is increased) or a combined vaporous-ventilated supercavity. Moreover,

1. **Test section,** 1.20m x 0.19m x 0.19m
2. **Test section dome**
3. **Skimmer**
4. **7° diffuser**
5. **Guide vane elbow**
6. **Axial flow pump, 150 HP**
7. **Diffuser screens**
8. **Gas collector dome**
9. **Gas separator, 2134D**
10. **Honeycomb**
11. **Contraction**
12. **Nozzle**
13. **Settling Chamber**
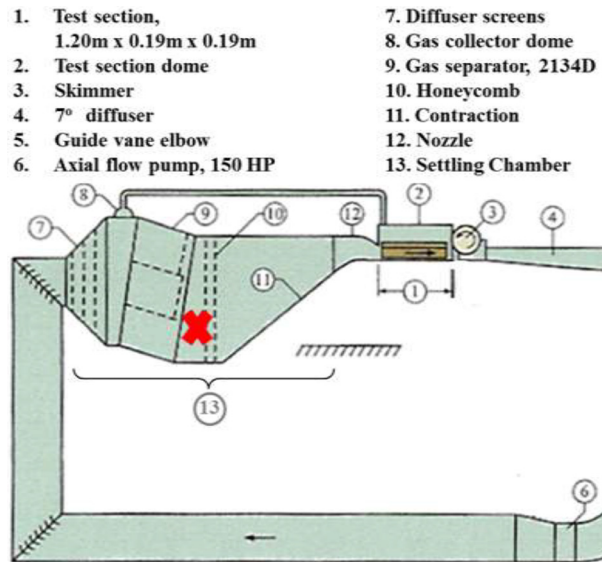
Fig. 1. Schematic of the test-section of the experimental facility along with the orientation of the two models in the test-section. The cross mark represents the location where temperature and dissolved oxygen concentration are measured in our experiments. Adapted from Karn et al. (2016a).

it must be pointed out that although a large number of studies have been conducted to study the steady developed cavities of ventilated and vaporous type, a systematic study of the supercavity formation process per se has not hitherto received much attention.

Thus, in the current study, we study the *formation process* of both the natural and artificial supercavity separately and also study the effect of one mode on the other. First, the formation of a natural supercavity and the effect of increasing amounts of ventilation on the σ_v requirements for supercavity formation (σ_{vf}) is explored. Next, C_{Qs} requirements for the formation of an artificial supercavity (C_{Qsf}) are explored and then its variation with respect to increasing amount of suppression of natural supercavitation is investigated. This paper is structured as follows: Section 2 provides the details for the experimental facility and the setup. Subsequently in Section 3, we present results and discussion on the formation requirements for a supercavity under both modes, which is followed by a final conclusion in Section 4.

2. Experimental setup and methodology

Experiments were conducted to study the formation of supercavitation under natural and artificial modes under different flow conditions. The experiments were carried out in the high-speed water tunnel at the Saint Anthony Falls Laboratory. This water tunnel is a closed recirculating facility with horizontal test-section having a hydraulic diameter of 214 mm and dimensions of 1.20 m (Length) × 0.19 m (Width) × 0.19 m (Height) as shown in Fig. 1. This tunnel is specifically designed for experiments on natural and ventilated cavitation and is capable of operating at a maximum velocity of 20 m/s (Karn et al., 2015b,c,d, 2016c).

Backward Facing Model (Karn et al., 2015a, 2016a) or Free Closure Model (Karn and Rosiejka, 2017) was used in our experiments. In the backward facing model, a thin NACA0012 hydrofoil strut is placed upstream of the cavitator to avoid the interaction between the formed cavity and the strut body leading to a free closure as reported by Logvinovich (1973). Fig. 2 demonstrates how the BFM is being mounted in the test-section.

To minimize the disturbance to the flow, the thickness of the hydrofoil strut is limited to 5 mm, so that it can barely envelope the ventilation pipe running to the cavitator. The hydrofoil has a
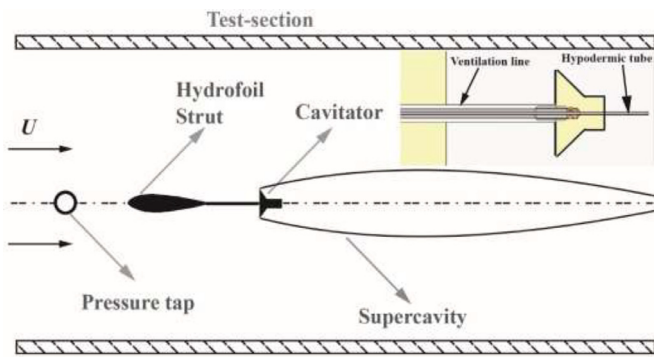
Fig. 2. Schematic showing the experimental model, backward facing model (BFM) being mounted in the test-section of the water tunnel. Inset shows a close-up view of the cavitator, with ventilation lines for gas injection and hypodermic tube for pressure measurement.
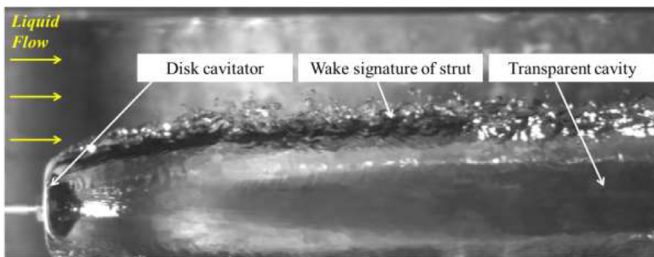
Fig. 3. A bottom view image of a supercavity obtained using BFM showing the influence of the preceding hydrofoil strut on the supercavity. The wake signature of the strut leaves only a minimal effect on the supercavity whereas the majority of the supercavity retains its clear interface.

chord length of 41 mm and length of the hydrofoil span is kept 190 mm so that it completely spans the test-section. Disk-type cavitator of 20 mm diameter is screwed at the end of the ventilation pipe. The angle of attack of the hydrofoil is measured between the axis of the test-section and the axis perpendicular to the flat surface of the disk cavitator, and is kept to 0° with a measurement accuracy of ±0.5°. The cavitator and the hydrofoil are made of brass and are polished to a smooth finish.

As per the suitability of BFM in our experiments, it may be argued that the upstream strut in the BFM may generate a turbulent wake, which may induce a significant perturbation of the flow near the cavitator, particularly on the separating flow at the edge of the cavitator where cavitation inception occurs. To assess the validity of this claim, systematically high speed videos of the supercavity are obtained. High speed videos of the supercavity under such a configuration reveal that the thin and streamlined hydrofoil strut upstream does not produce considerable disturbance, and only a slight wake signature is observed on the side of the cavity as also shown in the bottom view image of the supercavity in Fig. 3. It is indeed tempting to believe that locating the suspending strut downstream of the cavitator, either near the supercavity wake collapse or near the central portion of the supercavity may prove to be better choices for minimizing the interactions with the flow phenomena. To verify this hypothesis, another experimental model, Forward Facing Model (FFM) was tested, in which the cavitator precedes the hydrofoil strut. However, high speed videos of the supercavity formation process through FFM, particularly under the natural supercavitation mode showed that the individual vapor bubbles from the cavitator edge are liable to be destroyed upon collision with the ventilation pipe. Similarly, if the strut is placed closer to the cavitator such that the strut might pierce the supercavity, there is another fundamental problem with such an experimental setup. The bubbly cavity, just before the supercavity forma-

tion, interferes with the strut and thus has an unpredictable influence on the process of supercavity formation. Thus, it is coclusively established that BFM is most suited for studying the formation of supercavities.

Pressures in the test-section and the supercavity are measured using two separate Validyne absolute pressure transducers. A Validyne differential pressure transducer is employed to measure the differential pressure between the test-section and the settling chamber (see Fig. 1), and is used to calculate liquid velocity in the test-section. The pressure transducers are calibrated before each experiment using a mercury manometer. The pressure transducer calibrations are linear, with R-squared values typically 0.9999 or higher and the standard errors of the pressure calibrations are approximately 0.1 kPa for the pressure transducers. These errors cause a maximum error of 0.11 m/s in the measurement of velocity, with a mean error of about 0.02 m/s. Liquid flow speed in the test section is controlled through the rotational velocity of the tunnel's axial flow impeller which is driven with a 75HP AC motor. During the experiments, tunnel water temperature is monitored using a thermistor, and it varies between 16 °C and 20 °C over the course of the tests. A Hach luminescent dissolved oxygen (LDO) probe and controller is used to measure dissolved oxygen (DO) concentration in the settling chamber, and the measurements indicate that the dissolved oxygen concentration levels in the water of the test-section varied between 9.2 and 9.8 ppm for all the experiments. The images and the videos of the supercavity closure are obtained with a $1k \times 1k$ pixel Photon APX-RS camera, which is capable of acquiring 3000 frames/s at full resolution. To ensure uniform backlighting in these videos and images, a light shaping diffuser is placed between the light source and the flow.

The ventilation flow rate to the cavitator is controlled and measured by Omega Engineering FMA-2609A mass flow controller. In our experiments, gas flux is reported at the standard conditions (i.e. a temperature of 273 K and a pressure of 1 bar) in terms of standard liters per minutes (SLPM).The corresponding gas entrainment coefficient at standard conditions is defined as: $C_{Qs} = \dot{Q}_{As}/Ud_C^2$, where $\dot{Q}_{As}$ represents the gas ventilation flow rate at standard conditions as measured by the mass flow controller. The full scale reading of the mass flow controller is 55 SLPM and the uncertainty in the flow measurement is ±1% of the full scale reading. The maximum uncertainty in the measurement of C_{Qs}, Fr and σ_v are estimated to be 2%, 2% and 3%, respectively.

3. Results and discussion

In the current study, two different kinds of experiments are conducted: In the first category of experiment, C_{Qs} required for formation of supercavity is measured at fixed σ_v, and is termed as formation air entrainment coefficient, or C_{Qsf}. The second category of experiments pertain to the measurement of σ_v for supercavity formation, at a fixed C_{Qs}, and termed correspondingly as formation natural cavitation number, or σ_{vf}. However, it is realized that in the combined vaporous-ventilated cavitation experiments, when both the test-section pressure and ventilation flow rate are regulated, it is not easy to hold the σ_v constant, since the ventilated gas gradually leads to a pressure buildup in the tunnel. In such cases, the constant pressure in the test-section (and hence fixed σ_v) is ensured by manual adjustment of both ventilation and suction. As a result, the test-section pressure fluctuated within ±0.5 kPa of the desired value. It is worth pointing out here, that the data collection for C_{Qs} and σ_v is not done for any particular supercavity geometry across all cases. Instead, C_{Qsf} and σ_{vf} denote those values which are obtained at the instant of the supercavity formation, when the other parameter (σ_{vf} and C_{Qsf} respectively) is successively increased or decreased, respectively. It is crucial to describe the process of supercavity formation in order to de-
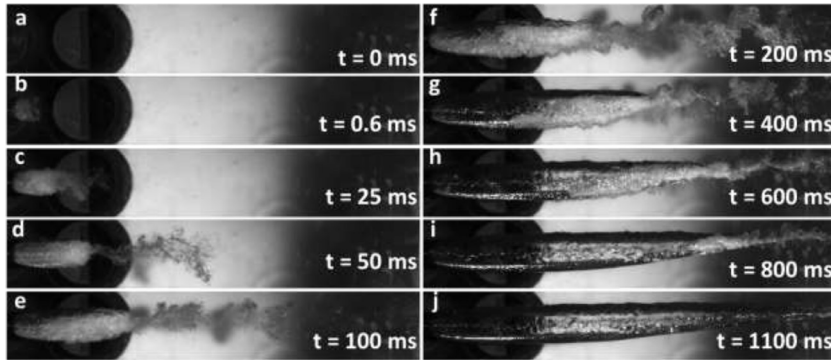
Fig. 4. Successive stages in the formation of a supercavity for BFM cavitator at $B = 9\%$, $Fr = 15.8$ and $C_{Qs} = 0.15$. (d) marks the inception of supercavitation and stages (g), (h), (i) and (j) correspond to the formed supercavities.

fine the criterion of inception of supercavitation. While increasing C_{Qs} or decreasing σ_v to form the supercavity, at each condition the experiment is steadily carried out and it is noted if a clear supercavity is formed. In our experiments, the supercavity is said to be formed if a clear interface has been established for at least half of the length of the supercavity. Fig. 4 presents the frames of a high speed video showing the process of supercavity formation at successive intervals of time, beginning from the stage of no gas ventilation at an initial time. As the figure shows, for a 20 mm disk cavitator ($B = 9\%$) and at a flow condition determined by $Fr = 15.8$ and $C_{Qs} = 0.15$, the process of supercavity inception (i.e. the occurrence of a clear interface) occurs after 50 ms. However, the supercavity rear portion is still covered with bubbly foam and supercavity can't be said to be established. However, after a duration of 400 ms or more, majority of the supercavity has a clear interface and the supercavity can be said to be established. Provided the gas entrainment is sufficient, the process of origination of a supercavity from the individual bubbles is a rapid one, transpiring on the scale of hundreds of milliseconds. Keeping this in mind, to study the supercavity formation process at each C_{Qs}, sufficient time was provided (5–10 s) for the flow to stabilize and coalescence processes to occur resulting in a clear supercavity. A conservative longer time gap was allowed, to also take into account the formation of supercavity through the natural supercavitation route, where the coalescence is of vapor bubbles, instead of gas bubbles.

3.1. Effect of ventilation on natural supercavitation

First, the effect of ventilation on natural supercavitation is explored. In a steady, fully developed natural cavity, the dissolved air and heat are both diffused through the liquid towards the interface, thereby leading to a continuous supply of air and vapor to the cavity. This is balanced by the rate of entrainment of volume of air and vapor away from the cavity in the wake (Brennen, 1969a). If air is deliberately blown into the supercavity, the cavity pressure is affected and the cavity must adjust itself in a way that wake entrains air from the cavity at a rate that balances the rate of feeding air into the cavity (Gadd and Grant, 1965). A pertinent question may be raised here as to the suitability of our experiments regarding the claim of 'a purely vaporous supercavity'. As described before, the presence of dissolved gases in the water makes the presence of air inside the supercavity unavoidable since it diffuses through the liquid and sets up a partial pressure. However, it must be noted that the current work does not pertain to the formed and steady supercavity per se, but the *process of formation of supercavities* via a bubble coalescence process. Hence, considering the nature of our experiments, the discussion on the formation of 'a purely vaporous supercavity' is well posed. In our experiments, the objective of the experiment is to first measure the σ_v at which a supercavity forms at a particular Fr and then study its variation as
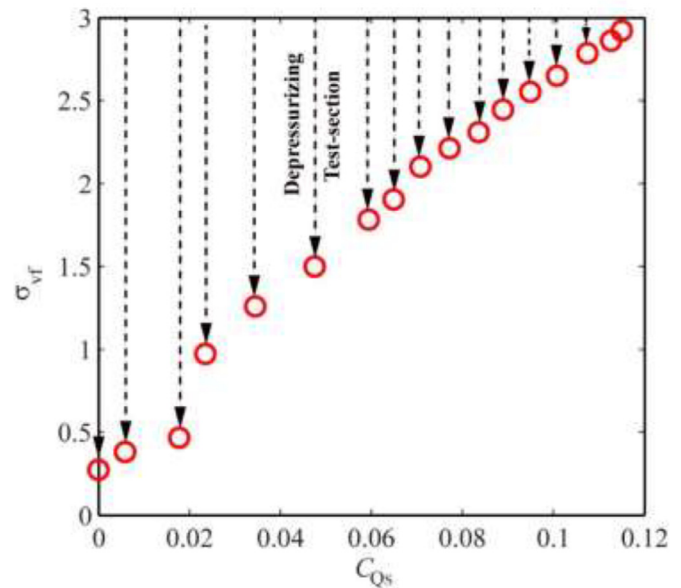
Fig. 5. Variation in natural cavitation number requirement for supercavity formation with respect to gas entrainment coefficient at $Fr = 15.8$. Natural cavitation number is varied solely by depressurizing the test-section. Downward arrows indicate that σ_v is lowered beginning from $\sigma_v = 3$, till a supercavity is formed.

some ventilation air is introduced. Fig. 5 presents the variation of vaporous cavitation number at which a supercavity is formed (σ_{vf}) with respect to increasing amounts of gas entrainment coefficient. The data was collected at each C_{Qs} (beginning from zero) by depressurizing the test-section pressure and changing the σ_v, till a supercavity is formed (i.e. σ_v approaches σ_{vf}). At a liquid velocity in the test-section corresponding to $Fr = 15.8$, the σ_v value corresponding to the test-section pressure is almost equal to 3 (referred hereafter as neutral pressure point, or NPP), and the formation of a supercavity necessitates that σ_v be lowered, and more and more cavitation bubbles be generated. As Fig. 5 shows, the formation of a purely natural supercavity (i.e. $C_{Qs} = 0$) is observed at a σ_{vf} as low as 0.25. However, as C_{Qs} gradually increases, a supercavity can be established at larger values of σ_{vf}, i.e. lesser reduction in test section pressure is required to establish a supercavity. Below a C_{Qs} of 0.02, no drastic increment in σ_{vf} requirement is seen. However, beyond a C_{Qs} of 0.02, there is a steep rise in the σ_{vf} requirements for establishing a supercavity and increases almost linearly. This trend can be explained thus: The rate of cavitation in the inception stage depends on σ_v and many other physical factors such as dissolved gas concentration, concentration of nuclei in the liquid, surface tension etc. As σ_v decreases, bubbles increase in number and coalesce further to produce larger size bubbles (Karn et al., 2016c;

Wu, 1972). When σ_v has dropped to a sufficiently low value, a single large cavity is formed in the wake enveloping a vapor-gas mixture of constant pressure. The origination of a natural supercavity thus, is solely a result of coalescence of individual vapor bubbles, which are generated by cavitation. However, when some ventilation gas is introduced, both cavitation and gas bubbles participate in the coalescence process through gas-vapor interaction and the resulting supercavity generation. At extremely low C_{Qs} ($C_{Qs} < 0.02$), the presence of vapor bubbles dominates and the supercavity generation is governed through a vaporous route. Thus, extremely low σ_v in the range of 0.25–0.4 is required to effect the formation of supercavity. However, upon further increase in C_{Qs}, the supercavity generation process is governed and dominated by ventilation route. Thus, greater the C_{Qs}, more the presence of gas bubbles and consequently lesser the requirement of bubbles formed due to vaporous cavitation to form a supercavity. Hence, there is almost a linear relationship between the requirements of σ_v for supercavity formation (i.e. σ_{vf}) and C_{Qs}.

It is worth mentioning here that for natural supercavitation studies, thermal effects at the cavity interface as a consequence of the evaporation rate of the liquid is indeed related to the entrainment of gas and/or vapor at the cavity closure. It is possible that thermal effects may cool the liquid-vapor interface and reduce the partial pressure of the vapor with respect to the isothermal value and thus might alter the development of supercavities. The intensity of thermal effects is determined by the dynamic balance between the convective and conductive heat transfer in the liquid towards the interface and the evaporation requirements induced by the entrainment of the vapor in the wake. The intensity and relevance of thermal effects crucially depend on the partial pressure of the vapor, and varies with the temperature of the liquid. But, the water vapor or heat balance analysis by Brennen (1969a) has established that such small temperature differences involved in the supercavity experiments are practically undetectable. Further, considering the fact that the current study focuses on the formation of supercavities and not the gas-vapor dynamics after supercavity generation, thermal effects have a diminutive role in our experiments and are thus not considered.

3.2. Effect of vaporous cavitation on ventilation requirements of artificial supercavitation

Next, the consequence of the occurrence of cavitation on artificial supercavitation is examined. In an artificial supercavitation experiment, a supercavity is generated primarily by dint of coalescence of individual gas bubbles. However, in a water-tunnel experiment with disk cavitator, particularly at large Fr, bubbles are also generated because of vaporous cavitation. Thus, to effectively study the influence of natural supercavitation on ventilation requirements of artificial supercavitation, natural supercavitation has to be increasingly suppressed by causing overpressure in the test-section. Thus, beginning from a NPP of almost 3, σ_v was increased by pressurizing the test-section and holding it at a constant value and at each σ_v, an attempt was made to establish a ventilated supercavity beginning from no ventilation. The gas entrainment value at which supercavity is formed is recorded (i.e. C_{Qs} approaches C_{Qsf}). As shown in Fig. 6, a nearly linear trend is observed in C_{Qsf} with respect to σ_v. As σ_v increases from a value of 2.9 to 4.2, C_{Qsf} correspondingly rises from 0.12 to 0.17. Thus, upon increment in σ_v, lesser is the contribution of vaporous bubbles, and hence a larger requirement of gas entrainment to generate gas bubbles that can generate a supercavity.

A very interesting trend becomes evident when both the previous findings are plotted on the same curve, as illustrated in Fig. 7. As the figure shows, on the both sides of the NPP, the test-section is either in underpressure or overpressure state, and
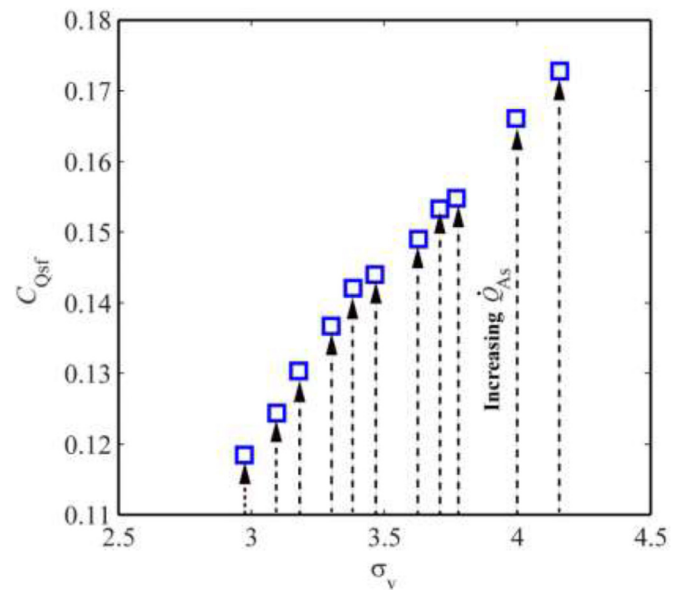
Fig. 6. Variation in gas entrainment requirement for supercavity formation with respect to natural cavitation number at $Fr = 15.8$. Larger values of σ_v were obtained by pressurizing the test-section. Upward arrows indicate that C_{Qs} is increased beginning from zero ventilation till a supercavity is formed.
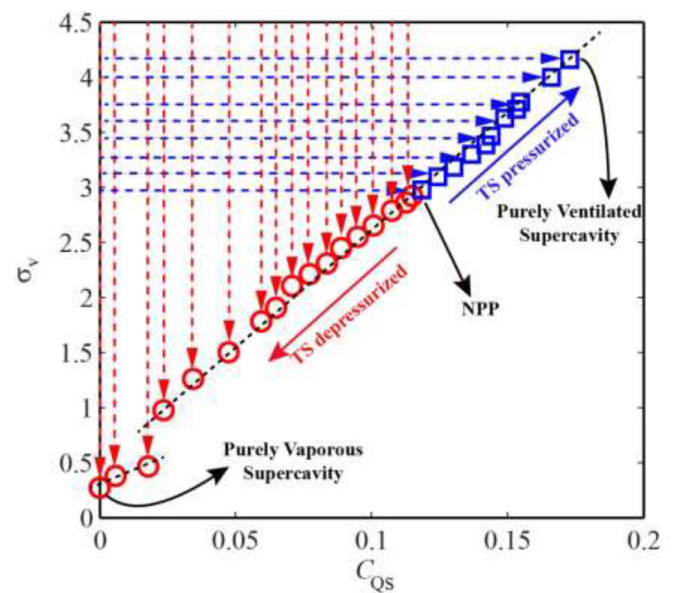
Fig. 7. Superposition of the $C_{Qs} - \sigma_{vf}$ and $\sigma_v - C_{Qsf}$ characteristics at $Fr = 15.8$. NPP refers to the neutral pressure point, i.e. a state when TS is neither pressurized nor depressurized. Horizontal and vertical arrows denote the way in which a supercavity is generated, either by decrement in σ_v or by increment in C_{Qs}. The black dotted lines indicate the slope of the two regions.

the supercavity is obtained through different modes. The point on the left extreme denotes a point of severe underpressure where only cavitation bubbles are formed which result in a purely vaporous supercavity. On the contrary, the point on the right extreme is that of excessive overpressure, with no cavitation bubbles being formed resulting in a purely ventilated supercavity. Further, the $C_{Qs} - \sigma_{vf}$ curve at $Fr = 15.8$ appears to be an extrapolation of the $\sigma_v - C_{Qsf}$ curve at the same Fr, indicating that there is something inherently similar between these two characteristic curves. The perfect continuity of these two curves, although obtained through different paths, is a strong indicator of the fact that the supercavity formation process is not hysteretic with respect to
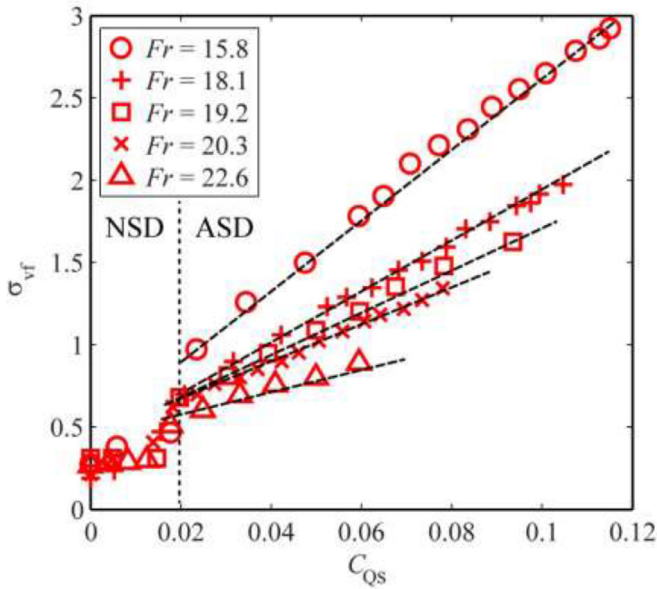
Fig. 8. $C_{Qs} - \sigma_{vf}$ characteristics at different Froude numbers. NSD and ASD regimes refer to Natural Supercavitation Dominated and Artificial Supercavitation Dominated regimes, respectively.

Fig. 9. $\sigma_v - C_{Qsf}$ characteristics at different Fr.

changes in σ_v or C_{Qs}. Thus, irrespective of the actual physical processes involved in the formation of a supercavity, the relationship between the non-dimensional parameters is identical.

3.3. Froude number effects

During the launch of an underwater vehicle, Froude numbers are typically low because of low velocity and ventilation is necessary. Usually, natural supercavitation occurs at large Froude numbers where the supercavity is axisymmetric and Froude number effects are negligible. A number of prior studies have focused upon the effect of Fr on the relationship of air entrainment and cavitation number (Campbell and Hilborne, 1958; Kawakami and Arndt, 2011). Many studies have also focused upon the effect of Fr upon the supercavity closure modes, and it has been proposed that the product of Fr and σ is a marker of the closure mechanism (Campbell and Hilborne, 1958; Spurk, 2002; Kawakami and Arndt, 2011). Since Fr is an important parameter governing supercavity formation, it has an important role in the formation of both ventilated and vaporous supercavity. The effect of change in Fr is investigated by plotting both the $C_{Qs} - \sigma_{vf}$ and $\sigma_v - C_{Qsf}$ characteristics at different Froude numbers, while keeping the blockage ratio constant, and only varying the flow speed. Fig. 8 presents the variation of σ_{vf} with respect to C_{Qs} for a range of Fr. Fr was held constant by fixing the liquid velocity in the test-section, and for each fixed value of C_{Qs}, the test-section pressure was regulated to change the values of σ_v. For all Fr tested, for a larger C_{Qs}, there is a linear $C_{Qs} - \sigma_{vf}$ relationship, which has been explained in the previous section. However, in the smaller range of C_{Qs}, $C_{Qs} - \sigma_{vf}$ variation is independent of Fr, and is nearly a constant. Although the exact reason behind such a trend is not completely clear, a plausible hypothesis can be proposed, considering the competing effects of a small amount of ventilation in a natural supercavity. The generation of a supercavity depends upon the nucleation and growth of a vapor bubble, as well as the growth of gas bubbles. According to Brennen (1969a), cavitation nuclei do not appear if the residence time of a fluid element in the region of low pressure is very small. If the residence time is sufficient for growth of cavitation nuclei, these may grow and coalesce to eventually generate a large cavity. It may then be hypothesized that a small amount
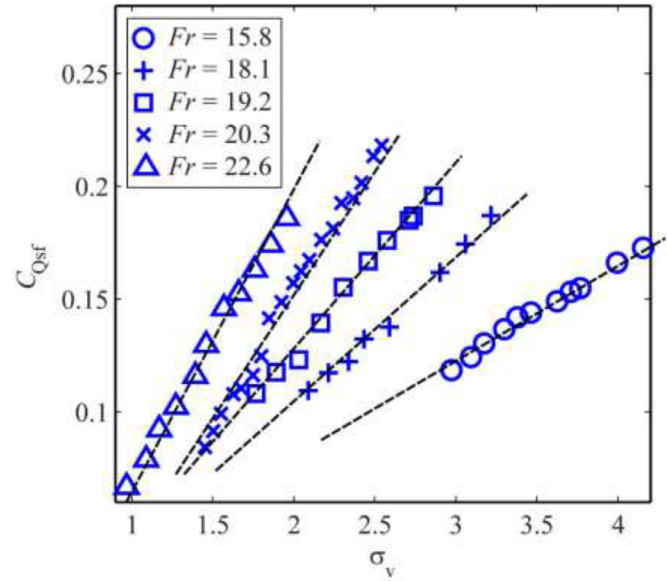
of ventilation, although favoring the coalescence of gas bubbles, may raise the cavity pressure sufficiently to eliminate the existence of a possible nuclei growth region very near to the cavitator rear portion (Brennen, 1969b). These competing effects may prevail and predominate in the range of low C_{Qs} ($C_{Qs} < 0.02$), where supercavity formation is predominated by the vaporous route (designated as NSD, or Natural Supercavitation Dominated) whereas for a larger C_{Qs}, the formation process of a supercavity is governed through the ventilation route (termed as ASD, or Artificial Supercavitation Dominated). Further, a quick evaluation of the slope of the curve $d\sigma_v/dC_{Qs}$ shows that the slope is inversely proportional to Fr, as can be seen from the Fig. 8. The variation in slopes at varying Fr can also be understood from another viewpoint in Fig. 9. Fig. 9 shows the variation of C_{Qsf} with σ_v at different Fr. As shown, for a fixed σ_v, C_{Qsf} increases as Fr increases. Recent studies have ascertained the dependence of C_{Qsf} on Fr and the reason behind such a dependence has been ascribed to the process of bubble coalescence (Karn and Rosiejka, 2017; Shao et al., 2017). On a similar note, it can be hypothesized here that greater Fr for the same cavitator size entails an increase in flow speed and turbulence, promoting more bubble breakup events. This in turn necessitates the requirement of a greater C_{Qsf} in order for the smaller bubbles to coalesce into a large supercavity.

3.4. Blockage effects

The effect of wall blockage in our experiments is captured by the blockage ratio (B), which is the ratio of the cavitator diameter and the hydraulic diameter of the water tunnel. Fig. 10 illustrates the effect of blockage on $C_Q - \sigma_{vf}$ characteristics. It shows that the change in blockage predominantly affects the initial characteristics in the NSD regime, while the later part of ASD regime remains largely the same. Evidently, the cavitation number requirements for the formation of a natural supercavity is dependent upon blockage at a fixed Fr. As the figure shows, a natural supercavity is formed at a σ_v of 0.21 and 0.41 at a blockage of 9% and 14%, respectively. As the blockage increases, σ_{vf} increases correspondingly and the NSD regime shifts to the left. This can be explained on the same basis that a lower blockage cavity allows for the attainment of lower cavitation numbers, as reported by prior studies (Kawakami and Arndt, 2011; Karn et al., 2016a). However, it is observed once there is a significant amount of gas entrainment
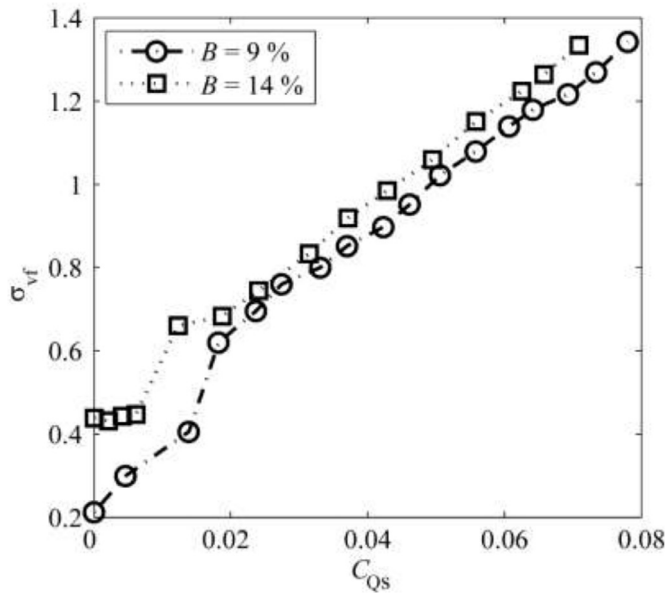
Fig. 10. The effect of blockage on $C_{Qs} - \sigma_{vf}$ curve at a fixed *Fr*.

resulting in the presence of gas bubbles in the flow (i.e. the ASD regime), the pressure reduction requirements (i.e. σ_v) are not very stringent with respect to blockage ratio. In summary, as suggested by the previous observations, there is a synergy between the ventilated cavitation and the natural cavitation for the formation of a supercavity.

4. Conclusions

Understanding of the synergistic relationship between vaporous and ventilated supercavitation is important, especially because the operation of a supercavitating underwater vehicle is driven by an interplay between these two distinct modes of supercavitation. It was pointed out that although a lot of prior studies have focused upon the study of steady and developed natural and artificial supercavities, the process of supercavity formation process has not been studied systematically. Hence, the current work discusses the phenomenon of supercavitation under two distinct modes of ventilated and vaporous supercavitation and the synergistic interrelationship between these.

First, the formation of a natural supercavity and the effect of increasing amounts of ventilation on the σ_v requirements for supercavity formation is explored. Next, C_{Qs} requirements for the formation of an artificial supercavity are explored and then its variation with respect to increasing amount of suppression of natural supercavitation is investigated. Our experiments indicate that the supercavity formation process is governed by the coalescence events of both cavitation bubbles as well as gas bubbles, when present. The supercavity formation can be dominated by either the natural supercavitation (NSD regime) or artificial supercavitation (ASD regime). It was hypothesized that the occurrence of cavitation nuclei is favored in a region of low pressure, and a little amount of ventilation can increase the cavity pressure inhibiting cavitation in the NSD regime. In a steady, fully developed natural cavity, the dissolved air and heat may both diffuse through the liquid towards the interface, thereby leading to a continuous supply of air and vapor to the cavity. Further, it was also found that the supercavity formation process is not hysteretic with respect to changes in σ_v or C_{Qs}. Thus, irrespective of the path taken to obtain a supercavity, the relationship between the σ_v and C_{Qs} is identical. It can be concluded that a comprehensive and complete picture of cavita-

tion would not only entail an understanding of the processes that entrain air out of the cavity at the wake, but also those processes which diffuse air into the cavity, when dissolved air is present in the liquid.

Supplementary materials

Supplementary material associated with this article can be found, in the online version, at doi:10.1016/j.ijmultiphaseflow.2018.03.015.

References

Brennen, C., 1969a. Some Viscous and other Real Fluid Effects in Fully Developed Cavity Flows. Cavitation State of Knowledge, ASME.

Brennen, C., 1969b. The dynamic balances of dissolved air and heat in natural cavity flows. J. Fluid Mech. 37 (1), 115–127.

Brennen, C.E., 2013. Cavitation and Bubble Dynamics. Cambridge University Press.

Campbell, I.J., Hilborne, D.V., 1958. Air entrainment behind artificially inflated cavity. In: Proceedings of the Second Symposium on Naval Hydrodynamics. Washington, USA.

Cao, L., Karn, A., Arndt, R.E.A., Wang, Z., Hong, J., 2017. Numerical investigations into the pressure distribution within a ventilated supercavity. J. Fluids Eng. 139, 021301-01–021301-08.

Cox, R., Clayden, W., 1956. Air entrainment at the rear of a steady cavity. In: Proceedings of the Symposium on Cavitation in Hydrodynamics. London, United Kingdom.

Epshtein, L.A., 1975. Developed cavitation flows, Reprinted with translation from. In: additions bybook. Epshtein, LA, Pearsall, J.S. (Eds.), Cavitation" Translated into Russian. Publishing House MIR, Moscow, Russia, pp. 73–103.

Gadd, G.E., Grant, S., 1965. Some experiments on cavities behind disks",. J. Fluid Mech. 23 (4), 645–656.

Karn, A., Arndt, R.E.A., Hong, J., 2015a. Dependence of supercavity closure upon flow unsteadiness. Exp. Therm Fluid Sci. 68, 493–498.

Karn, A., Arndt, R.E.A., Hong, J., 2016a. An experimental investigation into supercavity closure mechanisms. J. Fluid Mech. 789, 259–284.

Karn, A., Arndt, R.E.A., Hong, J., 2016b. Gas entrainment behaviors in the formation and collapse of a ventilated supercavity. Exp. Therm Fluid Sci. 79, 294–300.

Karn, A., Ellis, C., Arndt, R.E.A., Hong, J., 2015b. An integrative image measurement technique for dense bubbly flows with a wide bubble size distribution. Chem. Eng. Sci. 122, 240–249.

Karn, A., Ellis, C., Arndt, R.E.A., 2015c. Investigations into the turbulent bubbly wake of a ventilated hydrofoil: moving towards improved turbine aeration techniques. Exp. Therm Fluid Sci. 64, 186–195.

Karn, A., Monson, G., Ellis, C., Hong, J., Arndt, R.E.A., Gulliver, J.S., 2015d. Mass transfer studies across ventilated hydrofoils: A step towards hydroturbine aeration. Int. J. Heat Mass Trans. 87, 512–520.

Karn, A., Rosiejka, B., 2017. Air entrainment characteristics of artificial supercavities for free and constrained closure models. Exp. Therm. Fluid Sci. 81, 364–369.

Karn, A., Shao, S., Arndt, R.E.A., Hong, J., 2016c. Bubble coalescence and breakup in the turbulent bubbly wake of a ventilated hydrofoil. Exp. Therm. Fluid Sci. 70, 397–407.

Kawakami, E., Arndt, R.E.A., 2011. Investigation of the behavior of ventilated supercavities. J. Fluids Eng. 133 (9), 1–11 091305.

Lee, S.J., Kawakami, E., Karn, A., Arndt, R., 2016. A Comparative study on the behaviors of ventilated supercavities between experimental models with different cavitator configurations. Fluid Dyn. Res. 48, 45506–45517.

Logvinovich, G.V., 1973. Hydrodynamics of Free-Boundary Flows. Halsted Press.

Rashidi, I., Pasandideh-Fard, M., Passandideh-Fard, M., Nouri, N.M., 2014. Numerical and experimental study of a ventilated supercavitating vehicle. J. Fluids Eng. 136 (10), 101301.

Savchenko, Yu.N., Savchenko, G.Yu, 2012. Gas flows in ventilated supercavities. In: Supercavitation: Advances and Perspectives A Collection Dedicated to the 70th Jubilee of Yu. N. Savchenko. Springer Science & Business Media, pp. 115–126.

Semenenko, V.N., 2001. Artificial supercavitation: physics and calculation. Ukrainian Academy of Sciences. Kiev Inst of Hydromechanics.

Serebryakov, V.V., Arndt, R.E.A., Dzielski, J.E., 2015. Supercavitation: theory, experiment and scale effects. J. Phys.: Conf. Ser. 656 (1), 012169–012173.

Shao, S., Karn, A., Ahn, B.K., Arndt, R.E.A., Hong, J., 2017. A comparative study of natural and ventilated supercavitation across two closed-wall water tunnel facilities. Exp. Therm Fluid Sci. 88, 519–529.

Silberman, E., Song, C.S., 1961. Instability of ventilated cavities. J. Ship. Res. 5 (1), 13–33.

Skidmore, G., 2013. The Pulsation of Ventilated Supercavities. Pennsylvania State University Master of Science thesis. Department of Aerospace Engineering.

Spurk, J.H., 2002. On the gas loss from ventilated supercavities. Acta mechanica 155 (3), 125–135.

Wu, T., 1972. Cavity and wake flows. Annu. Rev. Fluid Mech. 4, 243–284.

Zhang, X.W., Wei, Y.J., Zhang, J.Z., Wang, C., Yu, K.P., 2007. Experimental research on the shape characters of natural and ventilated supercavitation. J. Hydrodyn. Ser. B 19 (5), 564–571.